of the neopentyl di(tertiary phosphine) derivatives (Table III) exhibit the expected singlet with coordination chemical shifts similar to those of the related di(tertiary phosphine) complexes.[15] The proton-decoupled phosphorus-31 NMR spectra of the neopentyl tri(tertiary phosphine) complexes (Pneo-Pneo-Pneo)$M(CO)_3$ (M = Cr, Mo) and [(Pneo-Pneo-Pneo)NiCl][PF_6] exhibit the expected low-field triplet from the ligand center phosphorus atoms and the expected higher field doublet from the two ligand outer phosphorus atoms with coordination chemical shifts and phosphorus–phosphorus coupling constants similar to those of the related tri(tertiary phosphine) complexes.[15] The proton-decoupled phosphorus-31 NMR spectra of the remaining neopentyl tri(tertiary phosphine) complexes (Pneo-Pneo-Pneo)$RhCl_3$ and [(Pneo-Pneo-Pneo)MCl][PF_6] (M = Pd, Pt) exhibit two singlets since the phosphorus–phosphorus coupling is below the resolution limits of the spectrometer. The decrease in phosphorus–phosphorus coupling constants between two phosphorus atoms in a five-membered chelate ring formed by a poly(tertiary phosphine) upon descending a column of the periodic table from nickel through palladium to platinum was observed in the previous phosphorus-31 NMR study.[15]

The platinum–phosphorus coupling constants $|^1J(Pt-P)|$ in the complexes [(Pneo-Pneo-Pneo)PtCl][PF_6] and [P(-Pneo)$_3$PtCl][PF_6] are readily determined from the satellites in their proton-decoupled phosphorus-31 NMR spectra. The $|^1J(Pt-P)|$ coupling constants for the center phosphorus atoms appear around 3115 ± 10 Hz which is within the 3024–3242-Hz range found for similar phosphorus atoms in the previous work.[15] The $|^1J(Pt-P)|$ coupling constants for the end phosphorus atoms in coordinating $P(CH_2CMe_3)_2$ groups appear around 2300 Hz which is slightly below the 2340-Hz values found for the $|^1J(Pt-P)|$ coupling constants of the end phosphorus atoms in coordinating $P(CH_3)_2$ groups.[15]

Acknowledgment. We are indebted to the Air Force Office of Scientific Research for partial support of this work under Grant AF-AFOSR-71-2000. We are also indebted to the National Science Foundation for a major equipment grant to the University of Georgia Chemistry Department toward the purchase of the Jeolco PFT-100 pulsed Fourier transform NMR spectrometer. We acknowledge the technical assistance of Mr. Courtney Pape in running the NMR spectra.

Registry No. *cis*-(Pneo-Pneo)$Cr(CO)_4$, 57396-30-2; *cis*-(Pneo-Pneo)$Mo(CO)_4$, 57396-31-3; *cis*-(Pneo-Pneo)$W(CO)_4$, 57396-32-4; *fac*-(Pneo-Pneo)$Mn(CO)_3Br$, 57396-33-5; *fac*-(Pneo-Pneo)$Re(CO)_3Br$, 57396-34-6; *cis*-(Pneo-Pneo)$NiCl_2$, 57396-35-7; *cis*-(Pneo-Pneo)$PdCl_2$, 57396-36-8; *cis*-(Pneo-Pneo)$PtCl_2$, 57396-37-9; [(Pneo-Pneo)$_2$Rh][PF_6], 57396-39-1; [(Pneo-Pneo)$_2RhCl_2$][PF_6], 57396-41-5; [(Pneo-Pneo)$_2RuCl_2$][PF_6], 57396-43-7; *fac*-(Pneo-Pneo-Pneo)$Cr(CO)_3$, 57396-44-8; *fac*-(Pneo-Pneo-Pneo)$Mo(CO)_3$, 57396-45-9; [(Pneo-Pneo-Pneo)NiCl][PF_6], 57396-47-1; [(Pneo-Pneo-Pneo)PdCl][PF_6], 57396-49-3; [(Pneo-Pneo-Pneo)PtCl][PF_6], 57396-51-7; (Pneo-Pneo-Pneo)$RhCl_3$, 57396-52-8; [P(-Pneo)$_3$NiCl][PF_6], 57396-54-0; [P(-Pneo)$_3$PdCl][PF_6], 57396-56-2; [P(-Pneo)$_3$PtCl][PF_6], 57396-58-4; (Pneo-Pneo)$Mo(CO)_3Br_2$, 57396-59-5; [(Pneo-Pneo)$W(CO)_4Br]^+$, 57396-60-8; [P(-Pm)$_3$NiCl][PF_6], 54823-46-0; (Pneo-Pneo)$W(CO)_3Br_2$, 57396-61-9; $C_7H_8Cr(CO)_4$, 12146-36-0; $C_7H_8Mo(CO)_4$, 12146-37-1; $Mo(CO)_6$, 13939-06-5; $W(CO)_6$, 14040-11-0; $Mn(CO)_5Br$, 14516-54-2; $Re(CO)_5Br$, 14220-21-4; $(PhCN)_2PtCl_2$, 14873-63-3; $[C_8H_{12}RhCl]_2$, 12092-47-6; $C_7H_8Cr(CO)_3$, 12125-72-3; $C_7H_8Mo(CO)_3$, 12125-77-8; $(PhCN)_2PdCl_2$, 14220-64-5.

References and Notes

(1) Part XIII: R. B. King, J. C. Cloyd, Jr., and R. H. Reimann, *J. Org. Chem.*, in press.
(2) Postdoctoral research associate, 1971–1974.
(3) Postdoctoral research associate, 1974–1975, on leave from the National Chemical Research Laboratory, South African Council for Scientific and Industrial Research, Pretoria, South Africa.
(4) R. B. King, P. N. Kapoor, and R. N. Kapoor, *Inorg. Chem.*, **10**, 1841 (1971).
(5) R. B. King, R. N. Kapoor, M. S. Saran, and P. N. Kapoor, *Inorg. Chem.*, **10**, 1851 (1971).
(6) R. B. King and M. S. Saran, *Inorg. Chem.*, **10**, 1861 (1971).
(7) R. B. King, J. A. Zinich, and J. C. Cloyd, Jr., *Inorg. Chem.*, **14**, 1554 (1975).
(8) R. B. King and J. C. Cloyd, Jr., *J. Am. Chem. Soc.*, **97**, 53 (1975).
(9) R. B. King, "Organometallic Syntheses", Vol. I, Academic Press, New York, N.Y., 1965.
(10) R. B. King, J. C. Stokes, and T. F. Korenowski, *J. Organomet. Chem.*, **11**, 641 (1968).
(11) E. W. Abel and G. Wilkinson, *J. Chem. Soc.*, 1501 (1959); R. J. Angelici and A. E. Kruse, *J. Organomet. Chem.*, **22**, 461 (1970).
(12) M. S. Kharasch, R. C. Seyler, and F. R. Mayo, *J. Am. Chem. Soc.*, **60**, 882 (1938); J. R. Doyle, P. E. Slade, and H. B. Jonassen, *Inorg. Synth.*, **6**, 218 (1960).
(13) J. Lewis, R. S. Nyholm, C. S. Pande, and M. H. B. Stiddard, *J. Chem. Soc.*, 3600 (1963).
(14) R. B. King, *J. Coord. Chem.*, **1**, 67 (1971).
(15) R. B. King and J. C. Cloyd, Jr., *Inorg. Chem.*, **14**, 1550 (1975).
(16) L. M. Venanzi, *Angew. Chem.*, **76**, 621 (1964).
(17) R. B. King and M. S. Saran, unpublished results, 1970–1971; R. B. King and J. C. Cloyd, Jr., unpublished results, 1974.
(18) W. Levason and C. A. McAuliffe, *Adv. Inorg. Chem. Radiochem.*, **14**, 173–253 (1972).
(19) J. Lewis and R. Whyman, *J. Chem. Soc.*, 5486 (1965).
(20) H. L. Nigam, R. S. Nyholm, and M. H. B. Stiddard, *J. Chem. Soc.*, 1806 (1960).
(21) J. R. Moss and B. L. Shaw, *J. Chem. Soc. A*, 595 (1970).
(22) R. Colton, *Coord. Chem. Rev.*, **6**, 269 (1971).
(23) R. Colton, G. R. Scollary, and I. B. Tomkins, *Aust. J. Chem.*, **21**, 15 (1968).
(24) R. B. King, *Inorg. Nucl. Chem. Lett.*, **5**, 905 (1969).
(25) J. R. Gollogly, C. J. Hawkins, and J. K. Beattie, *Inorg. Chem.*, **10**, 317 (1971).

Contribution from the Department of Chemistry, University of Leuven, B-3030 Heverlee, Belgium

Charge-Transfer Spectra of Tetrahedral Transition Metal Complexes

L. G. VANQUICKENBORNE* and E. VERDONCK

Received October 6, 1975 AIC50727Q

A simple model is proposed for the description of charge-transfer states in transition metal complexes. The electron repulsion effects in the LMCT excited states are evaluated by using ligand field data. Indeed, the relative energies of certain excited CT states in a d^n system can be related to the ligand field levels of the corresponding d^{n+1} central ion complexes. The applicability of the proposed scheme is tested and demonstrated by studying the charge-transfer absorption spectra of a number of tetrahedral compounds, leading to a coherent interpretation of the spectral data.

I. Introduction

It is the purpose of this paper to make a few general remarks on the study of charge-transfer states in transition metal complexes. Important progress in this field has been made by Jorgensen,[1,2,19,24] Day, DiSipio, Oleari,[3–5] Gray,[6] and many others. Most of the work of these authors centers on a one-electron description, either in terms of optical electronegativities or in terms of a simplified molecular orbital theory. Only in a limited number of cases has the attention been focused on electron repulsion effects. Apparently, the theory

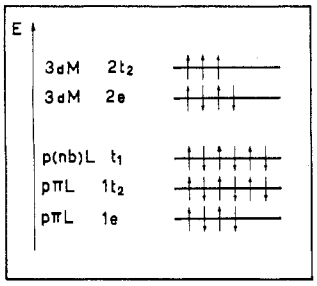

Figure 1. Partial molecular orbital energy level diagram for a tetrahedral d^7 system. The ligand σ orbitals are not included; they are probably too low in energy to be of importance in the assignment of the relevant bands.

of charge-transfer transitions has not reached the same degree of sophistication as the theory of the so-called "intra-metal" d–d transitions.

As an example, let us consider the well-known tetrahedral cobalt(II) tetrahalides. Figure 1 shows an approximate molecular orbital energy level diagram. The upper occupied orbitals 2e and $2t_2$ are antibonding and predominantly metal centered; the different transitions corresponding to a $2e \rightarrow 2t_2$ jump are d–d transitions within the seven-electron metal system. The other three orbitals are predominantly centered on the four halogen ligands; t_1 is a nonbonding ligand group orbital, while $1t_2$ and 1e are essentially π-bonding orbitals. An electron transfer from any one of these three orbitals to $2t_2$ can be considered to have charge-transfer character.

The ground state of this type of compound is $^4A_2$. The different excited charge-transfer states have the configuration $(2e)^4(2t_2)^4$ supplemented by one hole in the ligand orbitals. Each one of the three different excited configurations gives rise to a number of states, separated by electron repulsion and spin–orbit coupling. The latter effect being the smaller one, the main problem resides in the description of the electron repulsion effects.

II. A Simplified Model

In the evaluation of the repulsion integrals, one has to distinguish between integrals containing only the highest occupied $2t_2$ orbitals and integrals containing these $2t_2$ orbitals, as well as one of the three lower orbitals. The former integrals can be considered as a measure for the repulsion between two electrons, both mainly localized on the metal; they might be called M–M repulsion integrals. The latter integrals can be considered as a measure for the repulsion between one electron, mainly centered on the metal, and another one, mainly localized on the ligands (M–L repulsion integrals). Because of their many-center nature, the exact evaluation of these integrals is not easy. However, it seems reasonable to suppose that the M–L integrals are a good deal smaller than the M–M integrals. If this assumption can be carried through far enough, the picture will simplify considerably. For instance in the case of the cobalt(II) tetrahalides, the state energy level diagram would be described approximately by Figure 2. Within any one configuration, the metal part, here $(2t_2)^4$, is considered first, and the splitting pattern, resulting from the M–M interactions, is shown in the middle of the figure. This problem should be manageable, since it is concerned with the crystal field level scheme of a d^8 system. The coupling of each of the resulting states with the hole, mainly centered on the ligands, would then give rise to a number of relatively closely spaced energy levels. Therefore, *the charge-transfer spectrum of a d^n system might be connected to the crystal field spectrum of the corresponding d^{n+1} system.*

Apart from its inherent plausibility, the here presented model is quite compatible with Jorgensen's utilization of the

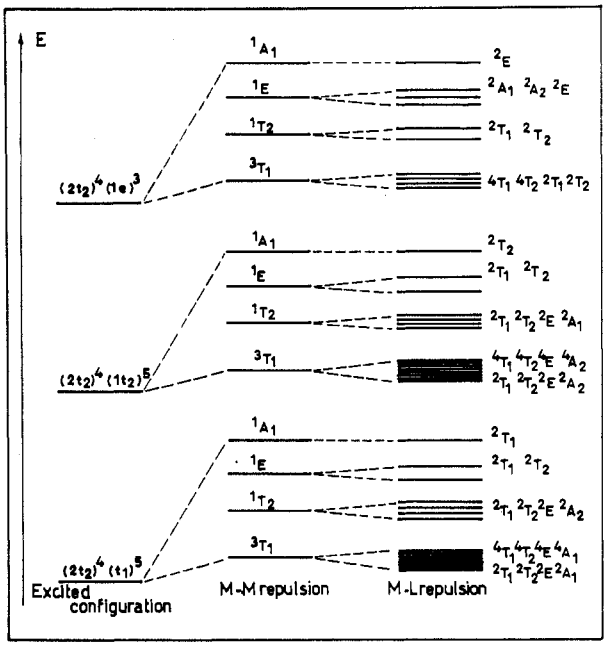

Figure 2. Qualitative energy level diagram for the charge-transfer excited states in CoX_4^{2-} complexes (X = halogen).

spin-pairing energy concept.[2] Jorgensen added this energy as a correction to his one-electron formula containing the orbital electronegativities of the metal and the ligands. The spin-pairing energy is a function of the spin quantum numbers of only the parent metal configuration; therefore, it really implies a weak coupling between the ligand hole and the partly filled metal subshell.[3,7–9]

III. Applicability of the Model

The cobalt(II) tetrahalides cannot be used to test the validity of the model. Indeed, if one limits oneself to the electric dipole transition mechanism, the *only* excited states, accessible from the $^4A_2$ ground state, are $^4T_1$. From Figure 2, it follows that each excited configuration gives rise to one, and only one, $^4T_1$ state. Therefore, the splitting pattern of the figure will certainly not be expected to show up in the actual spectra of the tetrahedral Co(II) compounds.

It is possible, however, to draw qualitative energy level diagrams for all tetrahedral d^n systems ($n = 1, 2, \ldots, 9$) and to find out which ones would be suitable to explore the applicability of the simple considerations outlined in the previous section. Table I shows the result of such an analysis. For the Co(II) systems, the electron had to be transferred from a ligand orbital to the metal $2t_2$ orbital, since the metal 2e orbital was then fully occupied by four electrons. However, in general, of course, both orbitals, 2e and $2t_2$, can be the electron acceptors. The symbol a in the table means that each excited configuration contains only one state, which is accessible by the electric dipole transition mechanism; this was the case of the Co(II) d^7 systems and it is equally the case of d^9 systems such as Cu(II), and a few others as well. In the b1 complexes, the different accessible states all belong to the same parent metal term; therefore, in the present context, one expects the resulting energy splittings to be small and difficult to evaluate. In the b2 complexes, on the other hand, the different accessible states belong to *different* parent metal terms; in these systems, comparatively larger energy splittings are expected and, most importantly, these splittings should be traceable to the crystal field splittings of the corresponding d^{n+1} systems. The last column of the table shows a number of examples. In what follows, the attention will be focused on the b2 cases, namely, $3d^1$, $3d^2$, and $3d^6$ high-spin compounds.

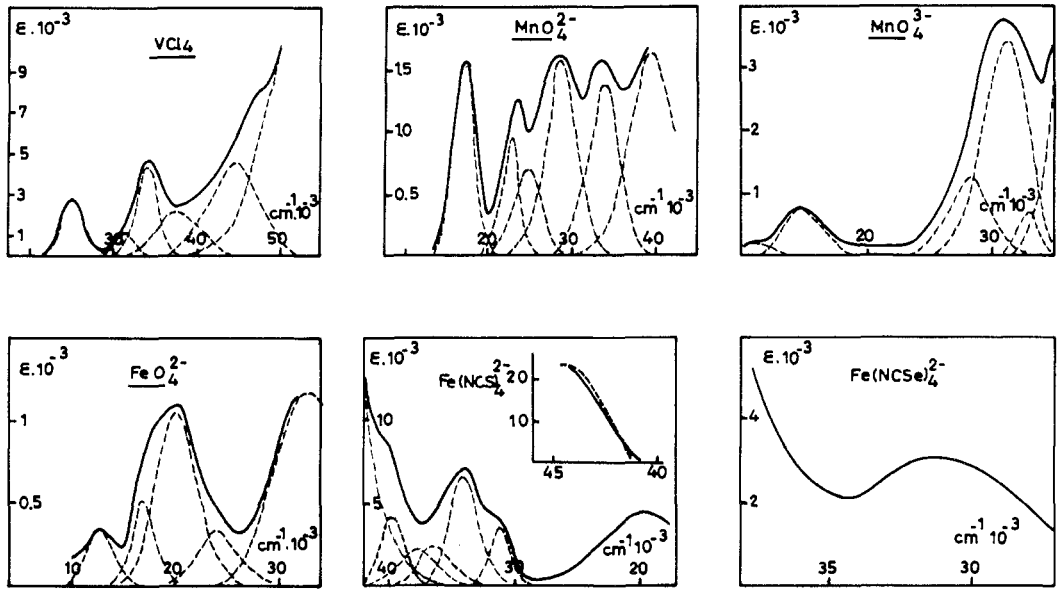

Figure 3. Gaussian analysis of the absorption spectra of a number of tetrahedral complexes.

Table I. Group Theoretical Analysis of the CT Excited States in All d^n Systems with T_d Symmetry[a]

System	2e acceptor	$2t_2$ acceptor	Example
d^1	b2	b2	VCl_4
			MnO_4^{2-}
d^2	a	b2	MnO_4^{3-}
			FeO_4^{2-}
d^3 high spin	b2	b2	
d^3 low spin	a	b2	
d^4 high spin	b2	b2	
d^4 low spin	*b*	a	
d^5 high spin	a	a	$FeCl_4^-$
			$FeBr_4^-$
d^5 low spin		b2	
d^6 high spin	a	b2	$Fe(NCS)_4^{2-}$
			$Fe(NCSe)_4^{2-}$
d^6 low spin		b2	
d^7		a	$CoCl_4^{2-}$
			$CoBr_4^{2-}$
d^8		b1	$NiCl_4^{2-}$
			$NiBr_4^{2-}$
d^9		a	$CuCl_4^{2-}$ [c]
			$CuBr_4^{2-}$ [c]

[a] The class to which a given complex belongs is given for the two possible acceptor levels 2e and $2t_2$. [b] 2e cannot be the acceptor level (completely filled). [c] Distorted T_d symmetry (D_{2d}).

IV. Specific Applications

A. Experimental Data. Figure 3 shows a Gaussian analysis of the absorption spectra of the following compounds: VCl_4, MnO_4^{2-}, MnO_4^{3-}, FeO_4^{2-}, $Fe(NCS)_4^{2-}$, and $Fe(NCSe)_4^{2-}$. The spectrum of VCl_4 refers to the gaseous state and was taken from Penella and Taylor.[10] From electron diffraction studies,[11] as well as infrared and Raman[12,13] spectroscopy, VCl_4 appears to have a regular tetrahedral structure. The MnO_4^{2-} spectrum is taken from den Boef et al.[14] There is a strong resemblance between the solution spectrum and the spectra of the same compound doped in M_2SO_4 (M = K, Rb, Cs).[4,5] Since the coordination in the solid state is very nearly T_d, there is a good reason to assume the same symmetry in solution. The spectra of MnO_4^{3-} and FeO_4^{2-} were taken from Johnson et al.[15] and Carrington et al.,[16] respectively.

As a result of the Gaussian analysis the position and in some cases also the number of absorption bands can be slightly different from what is indicated in the literature.

The $Fe(NCS)_4^{2-}$ and $Fe(NCSe)_4^{2-}$ spectra were measured in our laboratory on a Cary 14 in dichloromethane. The complexes were synthesized as described in the literature.[17,18] Although the synthesis was carried out under nitrogen atmosphere, EDTA titration indicated that part of the Fe(II) was probably oxidized to Fe(III); the spectral consequences of this fact will be discussed later. X-ray and ir studies[17,18] reveal a tetrahedral structure with N as the coordinating atom.

B. Theoretical Considerations. (1) Energies. For the different metal ions under consideration, the spin–orbit coupling constant is at most 400 or 500 cm^{-1}; therefore, in what follows, spin–orbit coupling will be neglected.

In the study of the optical properties of the tetrahedral complexes, the relevant orbitals are the ones shown in Figure 1. The energy difference between 2e and $2t_2$ is equal to the crystal field parameter $10Dq$. The relative order of the t_1, $1t_2$, and 1e orbitals does not seem to be altered in going from one tetrahedral complex to another.[3,19-21]

The consecutive introduction of M–M and M–L repulsions in T_d d^1 systems leads to a qualitative energy level diagram as shown in Figure 4. Both 2e and $2t_2$ can serve as acceptor levels. In each case, the different CT excited states, that are accessible by the electric dipole transition mechanism, are separated by M–M interactions. The energy differences for the corresponding d^2 systems are given—for the $(2e)^2$ configuration—by

$$E(^1A_1) - E(^1E) = 8B + 2C$$
$$E(^1E) - E(^3A_2) = 8B + 2C$$

and for the $(2e)^1(2t_2)^1$ configuration by

$$E(^1T_1) - E(^1T_2) = 4B$$
$$E(^1T_2) - E(^3T_1) = 2C - 4B$$
$$E(^3T_1) - E(^3T_2) = 12B$$

The energy difference between $^3T_2(2e)^1(2t_2)^1$ and $^3A_2(2e)^2$ is $10Dq$. The Racah parameters B and C might be taken directly from the experimental data of the d^2 complex; if this information is not available, they can be obtained from the free-ion parameters B_0 and C_0, multiplied by the nephelauxetic ratio β. The β values either can be found directly in the literature or can be estimated by interpolation or extrapolation of literature data.[1,19,22-24] The values of B_0, C_0, β, and the

Table II. Theoretical Crystal Field Splittings in the Excited CT States of T_d Complexes[a]

d¹ Systems

Complex	B_0	C_0	β	$8B+2C$	$4B$	$2C-4B$	$12B$
VCl_4	0.86	3.12	0.65	8.53	2.24	1.81	6.72
MnO_4^{2-}	1.45	5.76	0.40	9.26	2.33	2.28	6.98

d² Systems

Complex	B_0	C_0	β	$8B+2C$	$4B$	$6B+3C$
MnO_4^{3-}	0.96	3.98	0.45	7.04	1.73	7.97
FeO_4^{2-}	1.06	4.47	0.40	6.98	1.70	7.91

d⁶ Systems (High Spin)

Complex	B_0	β	$12B$	Complex	B_0	β	$12B$
$Fe(NCS)_4^{2-}$	0.75	0.8	7.17	$Fe(NCSe)_4^{2-}$	0.75	0.8	7.17

[a] The energies are expressed in kK.

Table III. Analytical Expressions for the Molecular Orbitals in T_d[a]

$$|2e\epsilon\rangle = c_1 d_{x^2-y^2} + c_2[1/2(y_1 - y_2 - y_3 + y_4)]$$

$$|2e\theta\rangle = c_1 d_{z^2} + c_2[1/2(x_1 - x_2 - x_3 + x_4)]$$

$$|1t_2\alpha\rangle = c_1' d_{yz} + c_2' x + c_3'[1/2(z_1 - z_2 + z_3 - z_4)] + c_4'[1/2(s_1 - s_2 + s_3 - s_4)] + c_5'[1/4((x_1 + x_2 + x_3 - x_4) + 3^{1/2}(-y_1 - y_2 + y_3 + y_4))]$$

$$|1t_2\beta\rangle = c_1' d_{xz} + c_2' y + c_3'[1/2(z_1 + z_2 - z_3 - z_4)] + c_4'[1/2(s_1 + s_2 - s_3 - s_4)] + c_5'[1/4((x_1 - x_2 + x_3 - x_4) + 3^{1/2}(y_1 - y_2 + y_3 - y_4))]$$

$$|1t_2\gamma\rangle = c_1' d_{xy} + c_2' z + c_3'[1/2(z_1 - z_2 - z_3 + z_4)] + c_4'[1/2 s_1 - s_2 - s_3 + s_4)] - c_5'[1/2(x_1 + x_2 + x_3 + x_4)]$$

[a] x, y, and z stand for p_x, p_y, and p_z; α, β, γ, ϵ, and θ are the components of the different spatial functions. The $2t_2$ orbitals have the same form as the $1t_2$ orbitals, but the coefficients c_1', c_2', c_3', c_4', and c_5' are replaced by c_1'', c_2'', c_3'', c_4'', and c_5''.

calculated energy splittings are given in Table II. The data for the d² and d⁶ systems are equally shown in the same table. The corresponding energy level[25] diagrams are shown in Figures 5 and 6. For the d² compounds, the energy difference between $^4T_1(2e)^2(2t_2)^1$ and $^2E(2e)^3$ equals $10Dq - 4B - 4C$. In the case of the d⁶ high-spin Fe(II) complexes, the energy difference between $^4T_2(2e)^3(2t_2)^4$ and $^4A_2(2e)^4(2t_2)^3$ equals $10Dq$.

(2) Intensities. From Figures 4–6, it appears that one given parent metal term gives rise to several accessible charge-transfer states. An analysis of the relative values of the intensities of these different transitions will obviously be very useful in the assignment problem.

In the Td systems under consideration, the states are to be described by (two or more)-open-shell configurations. Griffith's irreducible tensor method[26] allows one to calculate the different many-electron matrix elements in terms of a few one-electron matrix elements. In the Appendix, Griffith's method is extended so as to include three open shells.

Figure 7 and Table III show the coordinate system, the atom numbering, and the analytical MO expressions we have used. Qualitatively, it is obvious that the absolute values of c_1, c_1'', and c_5', will be the largest ones, say between 0.80 and 0.95, while all other coefficients will be a good deal smaller.

In the explicit evaluation of the one-electron transition moment integrals, only the diagonal elements on the ligand atoms were considered. Indeed, several authors have shown[3,27-29] that these elements carry the most important contribution to the dipole moment. The results of the intensity calculations of the d¹, d², and d⁶ high-spin systems are shown in Table IV.

(3) Spectral Interpretation. (a) 3d¹ Complexes. The spectral data on VCl_4 and MnO_4^{2-} have been analyzed by several authors;[4,6,10,30-32] their identifications are summarized in Table V. In all but two cases, the spectral assignments were made on the basis of a one-electron energy picture. Carrington and Symons[31] assigned state labels—partly on the basis of EPR data—while DiSipio et al.[4] accounted for electron repulsion in a way, which is to some extent similar to the procedure outlined here.

The relevant orbital transitions are $t_1 \rightarrow 2e$, $t_1 \rightarrow 2t_2$, and $1t_2 \rightarrow 2e$; quite probably the other possible LMCT transitions

Table IV. Intensity Calculations for the CT Bands in T_d d¹, d², and High-Spin d⁶ Systems[a]

System	Orbital transition	Metal term	CT state	Dipole strength
d¹	$t_1 \rightarrow 2e$	$^3A_2$	$^2T_2$	$(3/4)(c_2)^2$
		^1E	$^2T_1$	$(1/4)(c_2)^2$
			$^2T_2$	$(1/4)(c_2)^2$
		$^1A_1$	$^2T_1$	$(1/4)(c_2)^2$
	$1t_2 \rightarrow 2e$	$^3A_2$	$^2T_1$	$(3/4)(c_2)^2(c_5')^2$
		^1E	$^2T_2$	$(1/4)(c_2)^2(c_5')^2$
			$^2T_1$	$(1/4)(c_2)^2(c_5')^2$
		$^1A_1$	$^2T_2$	$(1/4)(c_2)^2(c_5')^2$
	$t_1 \rightarrow 2t_2$	$^3T_2$	$^2T_1$	$(27/32)(c_5'')^2$
			$^2T_2$	$(9/32)(c_5'')^2$
		$^3T_1$	$^2T_1$	$(9/32)(c_5'')^2$
			$^2T_2$	$(27/32)(c_5'')^2$
		$^1T_2$	$^2T_1$	$(9/32)(c_5'')^2$
			$^2T_2$	$(3/32)(c_5'')^2$
		$^1T_1$	$^2T_1$	$(3/32)(c_5'')^2$
			$^2T_2$	$(1/32)(c_5'')^2$
d²	$t_1 \rightarrow 2e$	^2E	$^3T_1$	$(c_2)^2$
	$1t_2 \rightarrow 2e$	^2E	$^3T_1$	$(c_2)^2(c_5')^2$
	$t_1 \rightarrow 2t_2$	$^4T_1$	$^3T_1$	$2(c_5'')^2$
		b^2T_1	$^3T_1$	$(c_5'')^2$
		a^2T_1	$^3T_1$	0
		b^2T_2	$^3T_1$	0
		a^2T_2	$^3T_1$	0
High-spin d⁶	$t_1 \rightarrow 2e$	$^4A_2$	$^5T_2$	$(1/2)(c_2)^2$
	$1t_2 \rightarrow 2e$	$^4A_2$	$^5T_1$	$(1/2)(c_2)^2(c_5')^2$
	$t_1 \rightarrow 2t_2$	$^4T_2$	$^5T_1$	$(9/16)(c_5'')^2$
			$^5T_2$	$(3/16)(c_5'')^2$
		$^4T_1$	$^5T_1$	$(3/16)(c_5'')^2$
			$^5T_2$	$(9/16)(c_5'')^2$

[a] The dipole strength is given as a function of R^2 (R is the metal-ligand distance) and the MO coefficients of Table III.

Table V. Spectral Assignments of the CT Bands of VCl_4 and MnO_4^{2-} As Proposed by Previous Authors[a]

VCl_4

Position (ϵ)	Alder-dice[30]	Penella-Taylor[10]	Position (ϵ)	Alder-dice[30]	Penella-Taylor[10]
24.8 (2800)	$t_1 \rightarrow 2e$	$t_1 \rightarrow 2e$	40.0 (~2500)	$VOCl_3$?	$t_1 \rightarrow a_1$ (4s)
29.9	$VOCl_3$?		45.4 (~5000)		$1t_2 \rightarrow 2e$
33.9 (4500)	$t_1 \rightarrow 2t_2$	$t_1 \rightarrow 2t_2$	>50.0 (~12 000)		$1t_2 \rightarrow 2t_2$

MnO_4^{2-}

Position (ϵ)	Carrington-Symons[31]	Carrington-Jorgensen[32]	Viste-Gray[6]	DiSipio et al.[4]
12.02 (very small)	$2e \rightarrow 2t_2(^2T_2)$			
15.54 (1598)	$t_1 \rightarrow 2e(^2T_2)$	$2e \rightarrow 2t_2$?	$2e \rightarrow 2t_2$	$t_1 \rightarrow 2e(^2T_2)$
22.91 (1330)	$t_1 \rightarrow 2e(^2T_1)$	$t_1 \rightarrow 2e$	$t_1 \rightarrow 2e$	$t_1 \rightarrow 2e(^2T_2)$
~26.60				$t_1 \rightarrow 2e(^2T_1)$
28.48 (1630)	$t_1 \rightarrow 2t_2(^2T_2)$	$1t_2 \rightarrow 2e$?	$1t_2 \rightarrow 2e$	$t_1 \rightarrow 2t_2(^2T_2$ or $^2T_1)$
33.40 (1539)	$t_1 \rightarrow 2t_2(^2T_1)$			

[a] The band positions (in kK) and the molar extinction coefficients are given for each transition.

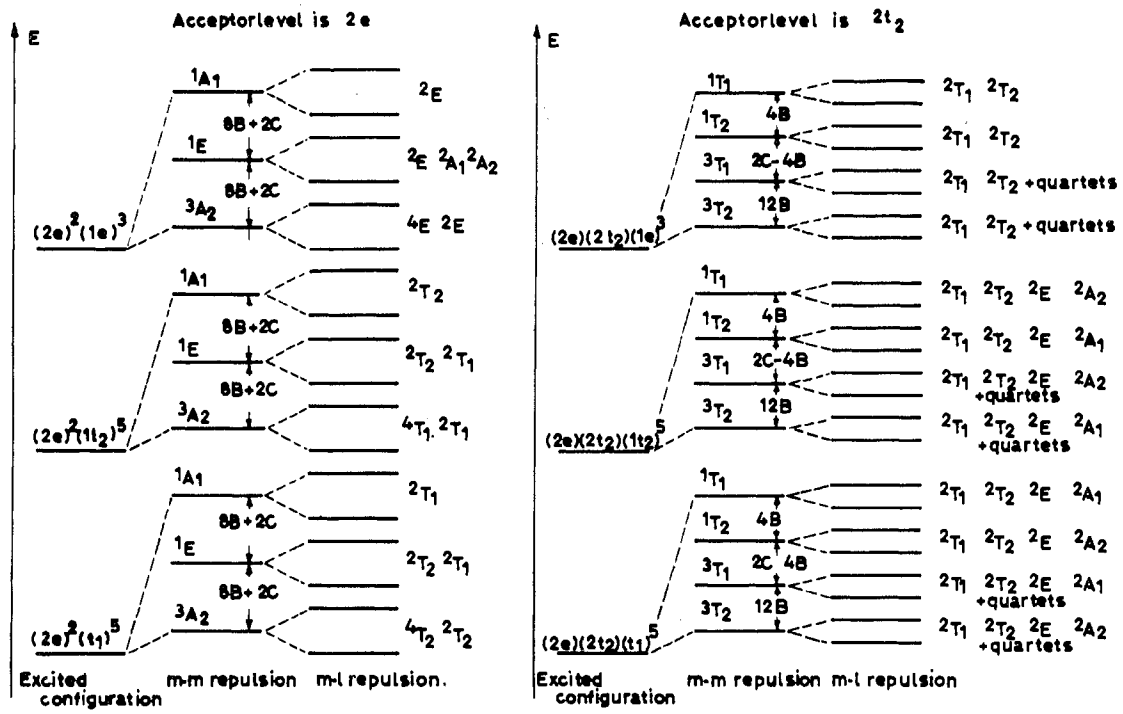

Figure 4. Qualitative energy level diagram for the charge-transfer excited states in T_d d^1 systems. The ground state is ^2E; the allowed transitions are $^2E \rightarrow {}^2T_1, {}^2T_2$.

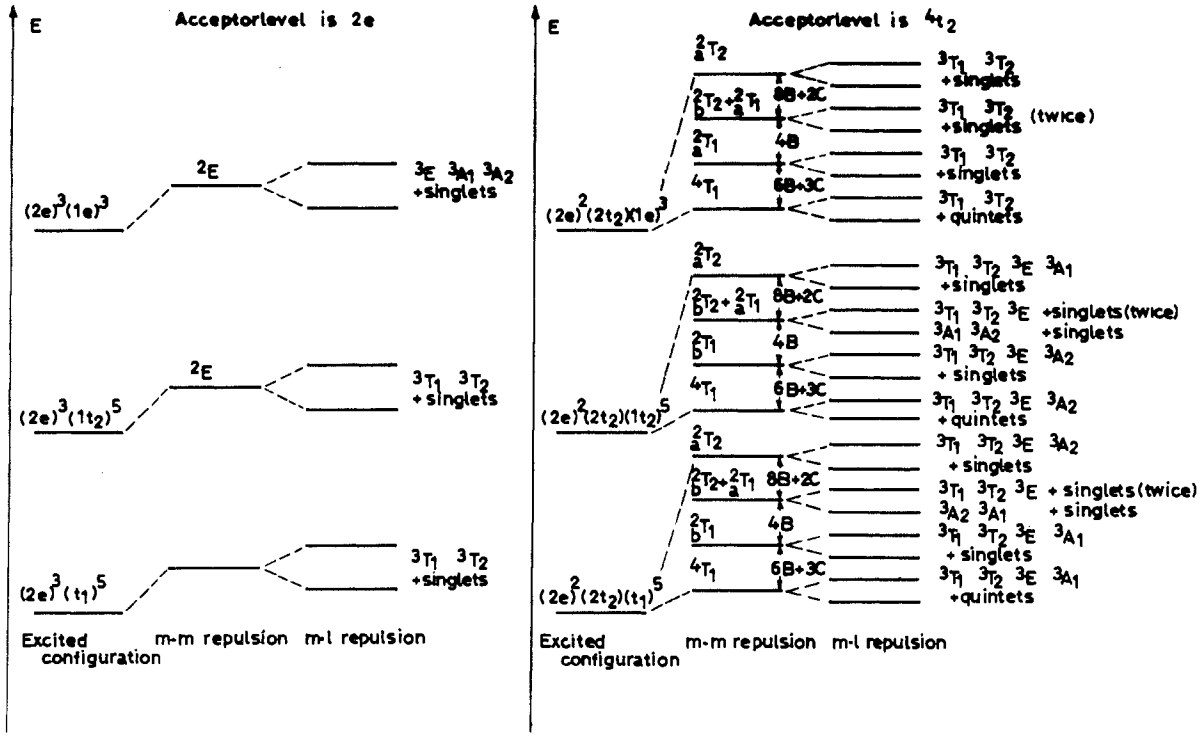

Figure 5. Qualitative energy level diagram for the charge-transfer excited states in T_d d^2 systems. The ground state is $^3A_2$; the allowed transitions are $^3A_2 \rightarrow {}^3T_1$.

fall outside of the spectral region under consideration. From Tables II and IV, it follows that t_1 and $1t_2 \rightarrow 2e$ should give rise to four bands, each with an intensity ratio 3:1:1:1. Within each group of four bands, the total energy splitting should be ~17 kK; one expects the two middle bands to be close together, both in energy and in intensity, with the most and the least energetic band each about 8 or 9 kK away. For the $t_1 \rightarrow 2t_2$ transition, Table IV predicts a rather complicated pattern of eight CT bands, subdivided into four sets of two, $^2T_1$ and $^2T_2$; within any one set, the energy splitting would be small, while the intensities would in all cases be in a ratio 1:3.

With this general framework in mind, it is possible to analyze and assign the spectra of VCl_4 and MnO_4^{2-} as in Table VI. The least energetic band in VCl_4 at 24.9 kK obviously corresponds to the $t_1 \rightarrow 2e$ orbital transition, more specifically leading to the excited $^2T_2$ ($^3A_2$) state where the parent metal term is written in parentheses. The transition at 31.1 kK is about 3 times less intense and is situated at about 6 kK from $^2T_2$ ($^3A_2$). It has therefore the properties expected for either

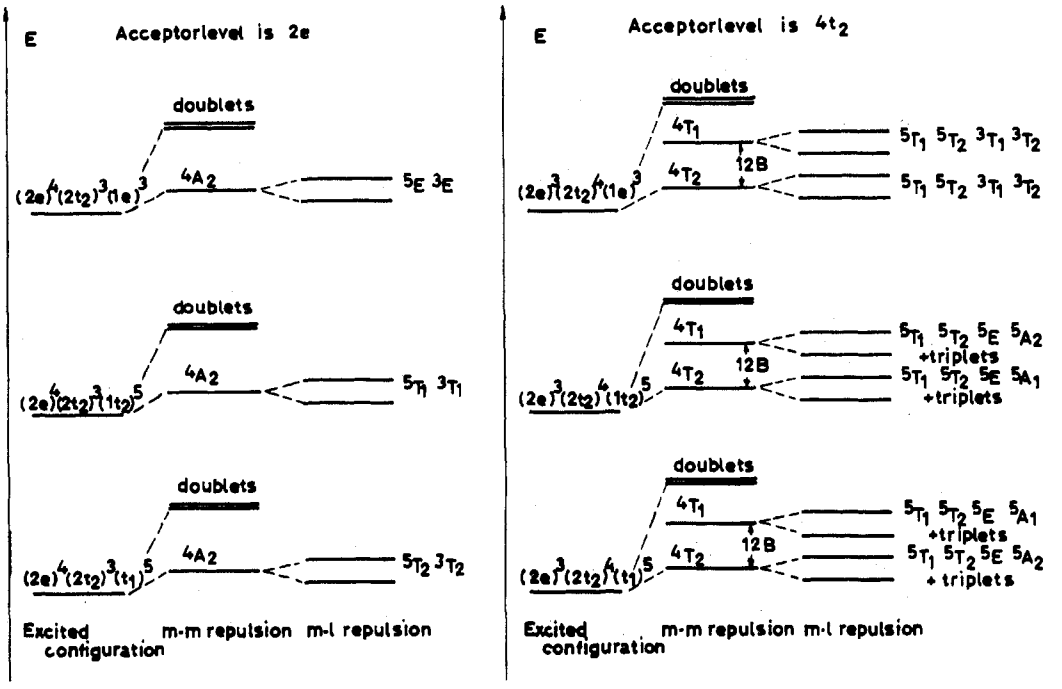

Figure 6. Qualitative energy level diagram for the charge-transfer excited states in T_d d^6 high-spin systems. The ground state is ^5E; the allowed transitions are $^5E \rightarrow {}^5T_1$, $^5T_2$.

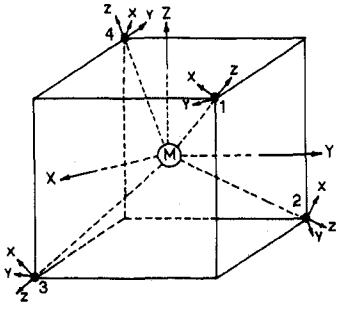

Figure 7. Coordinate system and atom numbering used in the calculation of the one-electron matrix elements.

$^2T_2$ (^1E) or $^2T_1$ (^1E); the present calculations do not provide us with an adequate criterion to distinguish between the two possibilities. In Table VI, the 31.1-kK band is assigned to the $^2E \rightarrow {}^2T_2$ transition, while the 33.7-kK band then corresponds to $^2E \rightarrow {}^2T_1$. The alternative assignment, obtained by interchanging the two CT states corresponding to the parent metal ^1E term, cannot be ruled out on the basis of our calculations. However, on the basis of single-crystal studies on the manganate ion, DiSipio et al.[4] found $^2T_2$ to be lower in energy than $^2T_1$. Therefore, in Table VI, the same energetic order was adopted. The energy of the band at 37.5 kK suggests the assignment $^2E \rightarrow {}^2T_1$ ($^1A_1$). The intensities remain a problem in this assignment, since the last two bands are clearly more intense than predicted. It seems reasonable to suppose that the set of bands, corresponding to the $t_1 \rightarrow 2e$ transitions, overlaps to some extent with another set of transitions. Probably this new set does *not* correspond to the orbital jump $t_1 \rightarrow 2t_2$. Indeed, if so, the spectrum would have a more complex structure. Moreover, if the 33.7-kK band is associated to the (close-lying) $^2T_1$ ($^3T_2$) and $^2T_2$ ($^3T_2$) states, the 37.5-kK band would have to be associated with the $^2T_1$ ($^3T_1$) and $^2T_2$ ($^3T_1$) states. While this is more or less acceptable on energetic grounds, Table IV predicts an equal intensity for these two sets of transitions; this is in conflict with the experimental data. Therefore it seems more reasonable to suppose that the overlapping orbital transition is $1t_2 \rightarrow 2e$. The $^2E \rightarrow {}^2T_2$ (^1E) component then overlaps with the $^2E \rightarrow$

Table VI. Interpretation of the CT Spectra of T_d d^1 Systems[a]

Position (ϵ)	Orbital transition	CT state (parent metal state)	Position (ϵ)	Orbital transition	CT state (parent metal state)
24.9 (2850)	$t_1 \rightarrow 2e$	$^2T_2$ ($^3A_2$)	16.7 (1560)	$t_1 \rightarrow 2e$	$^2T_2$ ($^3A_2$)
31.1 (4150)	$t_1 \rightarrow 2e$	$^2T_2$ (^1E)	22.5 (950)	$t_1 \rightarrow 2e$	$^2T_2$ (^1E)
33.7 (4150)	$t_1 \rightarrow 2e$ $1t_2 \rightarrow 2e$	$^2T_1$ (^1E) $^2T_1$ ($^3A_2$)	24.4 (710)	$t_1 \rightarrow 2e$	$^2T_1$ (^1E)
37.5 (2150)	$t_1 \rightarrow 2e$ $1t_2 \rightarrow 2e$	$^2T_1$ ($^1A_1$) $^2T_2$ (^1E)	28.1 (1560)	$t_1 \rightarrow 2e$ $1t_2 \rightarrow 2e$	$^2T_1$ ($^1A_1$) $^2T_1$ ($^3A_2$)
44.0 (4350)	?		33.1 (1340)	$1t_2 \rightarrow 2e$	$^2T_2$ (^1E)

[a] The band positions (in kK) and intensities (parentheses) are slightly different from the ones given in Table V, as a result of the Gaussian analysis of the spectra.

$^2T_1$ ($^1A_1$) of $t_1 \rightarrow 2e$, while the $^2E \rightarrow {}^2T_1$ ($^3A_2$) overlaps with the $^2E \rightarrow {}^2T_1$ (^1E) of $t_1 \rightarrow 2e$. Since c_5' is the π-bonding coefficient in the predominantly π-bonding $1t_2$ ligand orbital, it can roughly be put equal to 1; if so, summation of the theoretical intensities results in a ratio 3:1:4:2 for the first four bands. This is in very good agreement with the experimental data.

The identification of the bands in the MnO_4^{2-} spectrum can be made in a very similar way. On the whole, the CT spectrum will be shifted to smaller wavelengths with respect to VCl_4. Indeed, the optical electronegativity of V(IV) is 0.23 unit smaller than the optical electronegativity of Mn(VI), while the oxygen and chlorine ligands are at about the same place in the electronegativity scale.[19]

The first four bands result from the $t_1 \rightarrow 2e$ transition. The total energy splitting of these bands is smaller than in the VCl_4 case, but qualitatively, the pattern is identical. The overlapping with the $1t_2 \rightarrow 2e$ transitions now starts at the 28.1-kK band. De Michelis et al.[33] also pointed out the possibility of an overlapping between the different electronic configurations. The next transition at 33.1 kK is at 5 kK from the previous band; this is almost exactly the energy splitting between the $^3A_2$ and ^1E metal terms, as derived from the first four bands.

Table VII. Assignment of the Spectra of MnO_4^{3-} and FeO_4^{2-} As Proposed by Previous Authors

MnO_4^{3-}

Position (ϵ)	Carrington–Symons[31]	Carrington–Jorgensen[32]	Viste–Gray[6]	Kingsley et al.[34]	Orgel[35]
11.0 (small)			$2e \rightarrow 2t_2(^3T_2)$	$2e \rightarrow 2t_2(^3T_2)$	$2e \rightarrow 2t_2(^3T_2)$
14.8 (1100)	$t_1 \rightarrow 2e(^3T_1)$	$2e \rightarrow 2t_2$	$2e \rightarrow 2t_2(^3T_1)$	$t_1 \rightarrow 2e(^3T_1)$	$2e \rightarrow 2t_2(^3T_1)$
16.7 (small)				$2e \rightarrow 2t_2(^3T_1)$	
30.8 (3800)	$t_1 \rightarrow 2t_2(^3T_1)$	$t_1 \rightarrow 2e$	$t_1 \rightarrow 2e(^3T_1)$	$t_1 \rightarrow 2t_2(^3T_1)$	$t_1 \rightarrow 2e(^3T_1)$

FeO_4^{2-}

Position (ϵ)	Carrington-Symons[31]	Carrington-Jorgensen[32]	Viste-Gray[6]
12.8 (350)	$t_1 \rightarrow 2e(^3T_1)$	$2e \rightarrow 2t_2$	$2e \rightarrow 2t_2(^3T_2)$
17.7 (sh)			
19.6 (1120)	$t_1 \rightarrow 2t_2(^3T_1)$	$t_1 \rightarrow 2e$?	$2e \rightarrow 2t_2(^3T_1)$

Therefore, the bands are assigned as shown in Table VI.

An alternative interpretation, based on the overlapping of the $(1t_1)^5(2e)(2t_2)$ configuration, is less acceptable for the same reasons as in the VCl_4 case.

(b) $3d^2$ Complexes. Table VII shows the assignment of the MnO_4^{3-} and FeO_4^{2-} spectra, as proposed by previous authors.[6,31-35] The assignment of the CT bands was made on a one-electron basis in all cases.

It seems almost certain[6,34,35] that the first CT band lies at 28.4 kK and that it corresponds to the $t_1 \rightarrow 2e$ transition, i.e., $^3A_2 \rightarrow {}^3T_1$ (^2E). The extinction coefficient of the 31.6-kK band is at least 3 times too large to be associated with $1t_2 \rightarrow 2e$. This band corresponds more likely to the $t_1 \rightarrow 2t_2$, $^3A_2 \rightarrow {}^3T_1$ ($^4T_1$), transition, for which Table IV predicts an extinction coefficient of about 2000 or 3000 M^{-1} cm^{-1}. The 33.6-kK band cannot be associated with $^3A_2 \rightarrow {}^3T_1$ (b^2T_1), since this would require an anomalous value of $\beta = 0.12$ (Table II). However, it has both the energy and the intensity expected for the $1t_2 \rightarrow 2e$ transition.

The identification of the spectral bands of FeO_4^{2-} can be carried out in a very similar way. The assignments are summarized in Table VIII. It should be noticed that the first CT band of FeO_4^{2-} comes at much lower energy (11.4 kK) than in the MnO_4^{3-} spectrum. This can be expected on the basis of the difference in optical electronegativity (0.3 unit[19]) between Mn(V) and Fe(VI).

From Table VIII, it appears that the energy difference between the t_1 and $1t_2$ ligand orbitals does not change very much from one complex to the other (7 kK in the ferrate ion and 5.2 kK in the hypomanganate ion). The energy difference between the 2e and $2t_2$ metal orbitals can be calculated from the relative positions of the $^3T_1$ (^2E) and $^3T_1$ ($^4T_1$) levels and equals approximately 11.7 kK. This agrees fairly well with the $10Dq$ values derived from d–d spectra, 11.3 kK and 12.5 kK for MnO_4^{3-} and FeO_4^{2-}, respectively.[35]

(c) $3d^6$ High-Spin Complexes. Schmidtke[36] proposed a preliminary interpretation of the CT spectra of the iron(II) pseudohalides. He considered only the first band and identified it as the $t_1 \rightarrow 2e$ transition.

The $Fe(NCSe)_4^{2-}$ spectrum does not allow further analysis: it is almost completely structureless and shows only one very broad band at 32 kK. The $Fe(NCS)_4^{2-}$ spectrum on the other hand is well structured and deserves closer attention (Table IX). The least energetic band at 20 kK is most probably[37] due to $Fe(NCS)_6^{3-}$, which is formed very easily by oxidation. The first band of the $Fe(NCS)_4^{2-}$ complex lies at 31.8 kK and should of course be identified as $t_1 \rightarrow 2e$ or $^5E \rightarrow {}^5T_2$ ($^4A_2$). The next band at 34.3 kK is almost twice as intense as the first one, and, therefore, from Table IV, it should correspond not to $1t_2 \rightarrow 2e$ but rather to $t_1 \rightarrow 2t_2$, $^5E \rightarrow {}^5T_1$ ($^4T_2$). If the M–L interactions are small, the $^5E \rightarrow {}^5T_2$ ($^4T_2$) transitions should be at a few kilokaysers from the $^5T_1$ state with the same parentage; the intensity ratio for these two states should be 1:3. The 36.5-kK band satisfies these conditions. In this case—unlike the d^1 systems—the T_1 and T_2 states can be distinguished on the basis of their relative intensities.

The transitions at 38.5 and 40.1 kK have the right intensities to be associated with $^5E \rightarrow {}^5T_1$ ($^4T_1$) and $^5E \rightarrow {}^5T_2$ ($^4T_1$). However, this possibility should be rejected for two reasons. First, the band at 40.1 kK is probably[37] due to $Fe(NCS)_6^{3-}$. Second, this would imply an energy difference between the metal terms $^4T_1$ and $^4T_2$ of only about 4.5 kK, which is too small (β would have to be $\sim$0.5!). Therefore, the 38.5-kK band is associated with the $1t_2 \rightarrow 2e$ transition. The band at 44.2 kK is not identified; possibly, it is a ligand–ligand transition.[38]

The theoretical energy difference between the metal terms $^4T_2$ and $^4A_2$ equals $10Dq$. In the present context, the energy of the first CT band is a rough measure for the position of $^4A_2$, while the average of the second and the third band situates approximately $^4T_2$. This yields a $10Dq$ value of 3.6 kK, which is 70% of the value derived from the d–d spectrum.[17]

V. Conclusion

We proposed a general procedure which can be applied in the assignment of charge-transfer spectra of transition metal compounds. The spectra of a number of tetrahedral complexes have been analyzed and interpreted on the basis of two sets of results: first, ligand field calculations on the central ion, whose oxidation number is lowered by 1 unit, and, second, calculations of the relative transition probabilities. This implies that, as far as electron repulsion effects are concerned, the metal and the ligands can be considered as reasonably separate entities within the molecule.

A more quantitative agreement between theory and experiment would of course require the introduction of configuration interaction. However, even at the present level, the model seems to provide an adequate basis for the description of charge-transfer spectra.

Appendix. The Reduced Matrix Element of the Electric Dipole Operator between States Resulting from Three-Open-Shell Configurations

In the calculations of the intensities of the charge-transfer bands, it is necessary to evaluate the matrix elements of the dipole operator between states resulting from $a^m b^n c^o$ and $a^m b^{m+1} c^{o-1}$ configurations. Here, the "metal parts" $a^m b^n$ and $a^m b^{m+1}$ have to be coupled first, and, only then, are the "ligand parts" c^o and c^{o-1} coupled to the rest of the configuration.

It would be easier if a^m could be coupled to the rest, since in that case the problem could be solved by combining eq 10.15 and 10.19 of Griffith's book.[26] Indeed, in eq 10.15 b^n could be replaced by $b^n c^o$ in the bra and by $b^{n+1} c^{o-1}$ in the ket. If $b^n c^o$ and $b^{n+1} c^{o-1}$ give rise to $S_2 h_2$ and $S_2' h_2'$, respectively, the second g^n in eq 10.15 has to be replaced as follows

$$g^n{}_{h_2,h_2'}(b,f)\langle b\|u^f\|a\rangle \rightarrow \langle S_2 h_2 M_2\|U^f\|S_2 h_2' M_2\rangle$$

The latter reduced matrix element can then be evaluated from eq 10.19.

Therefore the remaining problem is one of changing the coupling order. In his eq 5.10, Griffith[26] gave a formula allowing a recoupling of functions, each characterized by one given irreducible representation of the molecular point group. If one has three functions A, B, and C, characterized at the same time by an irreducible representation for the space part and by a given set of spin quantum numbers, one finds

$$\left[\left(A^{S_1^a}_{h_1^a} \times B^{S_1^b}_{h_1^b}\right)^{S_1}_{h_1} \times C^{S_2}_{h_2}\right]^{SM}_{h\theta} =$$
$$(-1)^{h_1^a+h_1^b+h_2+h}(-1)^{S_1^a+S_1^b+S_2+S}(2S+1)^{1/2}\lambda(h_1)^{1/2} \times$$
$$\sum_{S_3,h_3}(2S_3+1)^{1/2}\lambda(h_3)^{1/2}\overline{W}\begin{pmatrix} S_1^b & S_1^a & S_1' \\ S & S_2 & S_3 \end{pmatrix} \times$$
$$W\begin{pmatrix} h_1^b & h_1^a & h_1 \\ h & h_2 & h_3 \end{pmatrix}\left[A^{S_1^a}_{h_1^a} \times \left(B^{S_1^b}_{h_1^b} \times C^{S_2}_{h_2}\right)^{S_3}_{h_3}\right]^{SM}_{h\theta}\Bigg]$$

where a and b are further specifications needed in the explicitation of the spin states; the configuration a^m leads to S_1^a, and b^n leads to S_1^b. The quantum number $S_3 = S_1^b + S_2$, $S_1^b + S_2 - 1$, ..., $|S_1^b - S_2|$, while h_3 is one of the irreducible representations in the direct product $h_1^b \times h_2$.

Using this expression, the reduced matrix elements of the electric dipole spectra in T_d, $U^f = R^{T_2} = \sum_k r(k)$, can be shown to be as in eq I.

$$\langle a^m(S_1^a h_1^a)b^n(S_1^b h_1^b)a^m b^n(S_1 h_1)c^o(S_2 h_2)SHM\|R^{T_2}\|\times$$
$$a^m(S_1^a{}' h_1^a{}')b^{n+1}(S_1^b{}' h_1^b{}')a^m b^{n+1}(S_1' h_1')c^{o-1} \times$$
$$(S_2' h_2')Sh'M'\rangle = \delta_{S_3 S_3'}\delta_{S_1^a S_1^a{}'} \times$$
$$(-1)^{h_1^b+h_2+h+h_1^b{}'+h_2'+h'+h_1^a+h_1^a{}'} \times$$
$$(-1)^{S_1^b+S_2+S_1^b{}'+S_2'+2S+2S_1^a} \times$$
$$(2S_1+1)^{1/2}\lambda(h_1)^{1/2}(2S_1'+1)^{1/2}\lambda(h_1')^{1/2} \times$$
$$\Bigg[\sum_{S_3,h_3}(2S_3+1)\lambda(h_3)\overline{W}\begin{pmatrix} S_1^b & S_1^a & S_1 \\ S & S_2 & S_3 \end{pmatrix} \times$$
$$\overline{W}\begin{pmatrix} S_1^b{}' & S_1^a & S_1' \\ S & S_2' & S_3 \end{pmatrix} W\begin{pmatrix} h_1^b & h_1^a & h_1 \\ h & h_2 & h_3 \end{pmatrix} \times$$
$$W\begin{pmatrix} h_1^b{}' & h_1^a{}' & h_1' \\ h' & h_2' & h_3' \end{pmatrix}\delta_{h_3 h_3'}(-1)^{T_2+h_2+h_3'}\lambda(h)^{1/2} \times$$
$$\lambda(h')^{1/2}(-1)^{h'} W\begin{pmatrix} h_1^a{}' & h_1^a & T_2 \\ h & h' & h_3 \end{pmatrix} \times$$
$$g^m{}_{h_1^a h_1^a{}'}(a,T_2)\langle a\|r^{T_2}\|a\rangle + \sum_{S_3,h_3,h_3'}(2S_3+1) \times$$
$$\lambda(h_3')^{1/2}\lambda(h_3)^{1/2}\overline{W}\begin{pmatrix} S_1^b & S_1^a & S_1 \\ S & S_2 & S_3 \end{pmatrix}\overline{W}\begin{pmatrix} S_1^b{}' & S_1^a & S_1' \\ S & S_2 & S_3 \end{pmatrix} \times$$
$$W\begin{pmatrix} h_1^b & h_1^a & h_1 \\ h & h_2 & h_3 \end{pmatrix} W\begin{pmatrix} h_1^b{}' & h_1^a & h_1' \\ h' & h_2' & h_3' \end{pmatrix} W\begin{pmatrix} h_3' & h_3 & T_2 \\ h & h' & h_1^a \end{pmatrix} \times$$
$$W\begin{pmatrix} S_1^b & S_2 & S_3 \\ S_2' & S_1^b{}' & 1/2 \end{pmatrix}\delta_{h_1^a h_1^a{}'}(-1)^{T_2+h_1^a+h_3'}\lambda(h)^{1/2} \times$$
$$\lambda(h')^{1/2}(-1)^h(-1)^{S_1^b+S_2'+S_3+1}(-1)^{h_1^b+h_2'+h_2+h_1^b{}'+T_2} \times$$
$$[(n+1)o(S_1^b{}'+1)]^{1/2}[(2S_2+1)\lambda(h_3)\lambda(h_3')\lambda(h_1^b{}')] \times$$
$$\lambda(h_2)]^{1/2}\langle b^n(S_1^b h_1^b),b\|\}b^{n+1}S_1^b{}'h_1^b{}'\rangle c^o(S_2 h_2) \times$$
$$\{\langle c,c^{o-1}(S_2' h_2')\rangle\langle c\|r^{T_2}\|b\rangle X\begin{pmatrix} h_1^b & h_2 & h_3 \\ h_1^b{}' & h_2' & h_3' \\ b & c & T_2 \end{pmatrix}\Bigg] \qquad (I)$$

Registry No. VCl_4, 7632-51-1; MnO_4^{2-}, 14333-14-3; MnO_4^{3-}, 14333-15-4; FeO_4^{2-}, 16836-06-9; $Fe(NCS)_4^{2-}$, 45069-78-1; $Fe(NCSe)_4^{2-}$, 57550-04-6.

Table VIII. Interpretation of the CT Spectra of T_d d^2 Systems: MnO_4^{3-} and FeO_4^{2-}

MnO_4^{3-}			FeO_4^{2-}		
Position (ϵ)	Orbital transition	CT state	Position (ϵ)	Orbital transition	CT state
28.4 (1200)	$t_1 \rightarrow 2e$	$^3T_1$ (^2E)	17.0 (500)	$t_1 \rightarrow 2e$	$^3T_1$ (^2E)
31.6 (3500)	$t_1 \rightarrow 2t_2$	$^3T_1$ ($^4T_1$)	19.9 (1100)	$t_1 \rightarrow 2t_2$	$^3T_1$ ($^4T_1$)
33.6 (800)	$1t_2 \rightarrow 2e$	$^3T_1$ (^2E)	24.0 (380)	$1t_2 \rightarrow 2e$	$^3T_1$ (^2E)

Table IX. Interpretation of the CT Spectrum of $Fe(NCS)_4^{2-}$

Position (ϵ)	Orbital transition	CT state	Position (ϵ)	Orbital transition	CT state
31.8 (3300)	$t_1 \rightarrow 2e$	$^5T_2$ ($^4A_2$)	36.5 (2500)	$t_1 \rightarrow 2t_2$	$^5T_2$ ($^4T_2$)
34.3 (6400)	$t_1 \rightarrow 2t_2$	$^5T_1$ ($^4T_2$)	38.5 (2200)	$1t_2 \rightarrow 2e$	$^5T_1$ ($^4A_2$)

References and Notes

(1) C. K. Jorgensen, "Modern Aspects of Ligand Field Theory", North-Holland Publishing Co., Amsterdam, 1971.
(2) C. K. Jorgensen, *Struct. Bonding (Berlin)*, **1** (1966).
(3) B. D. Bird and P. Day, *J. Chem. Phys.*, **49**, 404 (1968).
(4) L. DiSipio, L. Oleari, and P. Day, *J. Chem. Soc., Faraday Trans. 2*, **68**, 776 (1972).
(5) P. Day, L. DiSipio, G. Ingletto, and L. Oleari, *J. Chem. Soc., Dalton Trans.*, 2595 (1973).
(6) A. Viste and H. B. Gray, *Inorg. Chem.*, **3**, 1113 (1964).
(7) C. S. Naiman, *J. Chem. Phys.*, **35**, 323 (1961).
(8) J. C. Rivoal and B. Briat, *Mol. Phys.*, **27**, 1081 (1974).
(9) J. C. Collingwood, R. W. Schwartz, P. N. Schatz, and H. H. Patterson, *Mol. Phys.*, **27**, 1291 (1974).
(10) F. Penella and W. J. Taylor, *J. Mol. Spectrosc.*, **11**, 321 (1963).
(11) W. N. Lipscomb and A. G. Whittaker, *J. Am. Chem. Soc.*, **67**, 2019 (1945).
(12) J. A. Creighton, L. A. Woodward, and M. F. A. Dove, *Spectrochim. Acta*, **18**, 267 (1962).
(13) E. L. Grubb and R. L. Belford, *J. Chem. Phys.*, **39**, 244 (1963).
(14) G. den Boef, H. J. van der Beek, and T. Braaf, *Recl. Trav. Chim. Pays-Bas*, **77**, 1064 (1959).
(15) P. D. Johnson, J. S. Prener, and J. D. Kingsley, *Science*, **141**, 1179 (1963).
(16) A. Carrington, D. Schonland, and M. C. R. Symons, *J. Chem. Soc.*, 659 (1957).
(17) D. Forster and D. M. L. Goodgame, *J. Chem. Soc.*, 268 (1965).
(18) J. L. Burmeister and L. E. Williams, *Inorg. Chem.*, **5**, 1113 (1966).
(19) C. K. Jorgensen, *Prog. Inorg. Chem.*, **12** (1970).
(20) C. J. Ballhausen and H. B. Gray, "Molecular Orbital Theory", W. A. Benjamin, New York, N.Y., 1965.
(21) P. Ros and C. G. A. Schuit, *Theor. Chim. Acta*, **4**, 1 (1966).
(22) G. C. Allen and K. D. Warren, *Struct. Bonding (Berlin)*, **9** (1971).
(23) C. K. Jorgensen, "Oxidation States and Oxidation Numbers", Springer-Verlag, Berlin, 1969.
(24) C. K. Jorgensen, *Adv. Chem. Phys.*, **5** (1963).
(25) To the approximation used here, the metal terms a^2T_1 and b^2T_2 are degenerate. This approximation implies that the wave functions are constructed from the three terms resulting from $(2e)^2$. Second-order repulsion interactions between the two $^2T_1$ and the two $^2T_2$ states modify the energies by about 1 or 2 kK and lift the degeneracy. This effect does not fundamentally effect the applicability of the model.
(26) J. S. Griffith, "The Irreducible Tensor Method for Molecular Symmetry Groups", Prentice-Hall, London, 1962.
(27) C. J. Ballhausen and A. D. Liehr, *J. Mol. Spectrosc.*, **2**, 342 (1958).
(28) A. van der Avoird and P. Ros, *Theor. Chim. Acta*, **4**, 13 (1966).
(29) B. H. Wiers and W. L. Reynolds, *Inorg. Chem.*, **5**, 2016 (1966).
(30) D. S. Alderdice, *J. Mol. Spectrosc.*, **15**, 509 (1965).
(31) A. Carrington and M. C. R. Symons, *J. Chem. Soc.*, 889 (1960).
(32) A. Carrington and C. K. Jorgensen, *Mol. Phys.*, **4**, 395 (1961).
(33) G. De Michelis, L. Oleari, L. DiSipio, and E. Tondello, *Coord. Chem. Rev.*, **2**, 53 (1967).
(34) J. D. Kingsley, J. S. Prener, and B. Segall, *Phys. Rev. A*, **137**, 189 (1965).
(35) L. E. Orgel, *Mol. Phys.*, **7**, 397 (1963).
(36) H. H. Schmidtke, *Ber. Bunsenges. Phys. Chem.*, **71**, 1138 (1967).
(37) P. Day, *Inorg. Chem.*, **5**, 1619 (1966).
(38) J. R. McDonald, V. M. Scherr, and S. P. McGlynn, *J. Chem. Phys.*, **51**, 1713 (1969).